ELSEVIER

Burst resuspension of seabed material at the foot of the continental slope in the Rockall Channel

Jérôme Bonnin [*], Hans Van Haren, Phil Hosegood [1], Geert-Jan A. Brummer

Royal Netherlands Institute for Sea Research (NIOZ), P.O. Box 59, 1790 AB Den Burg, The Netherlands

Abstract

To better understand the relationship between near-bottom hydrodynamics and sediment resuspension in the transition zone between the continental slope and the abyssal plain, an array of three moorings equipped with near-bottom sediment traps and current meters was deployed in a triangular configuration of at the foot of the south-east slope of the Rockall Channel, North Atlantic. In addition a fast sampling ADCP was moored in the centre of the triangle. Microscopic observations combined with grain-size analysis revealed that the material intercepted by the traps was mainly composed of loose phytodetritus and aggregates. Organic carbon and $\delta^{13}C_{org}$ analyses further indicate that this material is relatively fresh and hence probably only transported over short distances. The total mass flux measured by the traps suggests input from either laterally advected or resuspended material during the deployment period. The measured flux was variable in time and space with a strong increase at the deepest site at the very foot of the slope. The measured flux did not correlate significantly with daily averaged current speed suggesting that processes other than those related to elevated bed shear stress are involved in the resuspension mechanism. Rapid changes in the hydrodynamics probably related to internal motions are evidenced by abrupt bursts in the current velocity and in the near-bottom turbidity. Their occurrence at slack tidal waters appears to be at the origin of the resuspension observed at the foot of the slope of the Rockall Channel. High resolution current velocity measurements suggest that resuspension is dominated by energetic, highly localised and short-term resuspension events, despite the abyssal depths. Part of these events resemble in many ways the solibores which have been previously observed to enhance sediment transport at much shallower depths over the continental slope while others rather appear to be associated to gravity waves.
© 2005 Elsevier B.V. All rights reserved.

1. Introduction

Continental slopes form a key area for the transfer of particles from the coastal area to the abyssal plain that is of major significance for carbon cycling on a global scale. Lateral advection of material from the adjacent shelf and sources on the slope appear far more important than the settling flux of primary particles produced in surface waters (Monaco et al.,

---

* Corresponding author. Present address: CEFREM, CNRS-Université de Perpignan, 66860 Perpignan cedex, France. Tel.: +33 4 68 66 22 48; fax: +33 4 68 66 20 96.
  E-mail address: jerome.bonnin@univ-perp.fr (J. Bonnin).
[1] Present address: Applied Physics Laboratory, University of Washington, 1013 NE 40th Street, Seattle, WA 98105, USA.

1990; Biscaye and Anderson, 1994; van Weering et al., 1998; Puig et al., 2001). Strong slope currents (Thomsen and van Weering, 1998, Durrieu de Madron et al., 1999) or internal waves impinging on the slope have been proposed as potential mechanisms for sediment resuspension and transport on the slope (Thorpe and White, 1988; Gardner, 1989; van Raaphorst et al., 2001; Cacchione et al., 2002). Results from oceanographic surveys carried out in the Faeroe–Shetland Channel in the framework of PROCS (Processes at the Continental Slope) showed that internal solibores caused abrupt changes in the current regime and in the suspended particle load near the bottom and facilitated sediment transport up the slope (Bonnin et al., 2002, 2005; Hosegood et al., 2004). Such short-term processes have a profound effect on the sedimentology and geochemistry of surface sediments (Bonnin and van Raaphorst, 2004) and are also thought to strongly influence the distribution of large epibenthic communities such as corals and sponges (Klitgaard et al., 1997).

Most studies aiming at understanding particle transfer to the deep-sea have concentrated on the shelf and upper slope (e.g., Durrieu de Madron et al., 1999; Puig et al., 2001; Palanques et al., 2002; McPhee-Shaw et al., 2004) where the sloping bottom is believed to favour generation of internal waves and further transport of sediments offshore via bottom and intermediate nepheloid layers. Few investigations, however, focussed on the processes responsible for particulate matter resuspension and transport in the transition zone between the abyssal plain and the base of the continental slope where the differences in topography are most pronounced. Assessing these processes is essential for our understanding of deep-sea ecosystems and ocean-margin exchange. To our awareness, little is known yet on the mechanisms involved in particle transport on the deep continental margins, particularly so with respect to the short-term mechanisms and spatial scales.

The present study was conducted as part of the NIOZ programme ROCS (ROckall Channel Studies) on the south-western slope of the Rockall Channel, and aimed at addressing the interactions between the hydrodynamics in the benthic boundary layer and the resuspension and transport of surface bottom sediment. In order to record rapid events and understand the associated short-term near-bottom hydrodynamics processes, we deployed, at nearly 3000 m water depth, an array of fast-sampling instruments as close as possible to the bottom to measure current velocity, turbidity and particle fluxes.

2. Characteristics of the study area

The present study was conducted down the southeast slope of the Rockall Channel (53°N, 14°W, Fig. 1). The axis of the channel is about 3000 m deep and the continental slope is relatively steep (up to 8%) with an abrupt transition with the flat abyssal plain. Between 2000–2800 m depth, 3.5 kHz ship's echo-sounder showed a rugged bottom topography (large boulders) with numerous gullies. The bottom slope ended abruptly and a weak slope (~0.5°) crossed the channel to the Rockall Bank due to filling of the basin by landslides during the Quaternary after large amounts of glacigenic material had been deposited (Stoker, 1995). Sediment input has been low since the last glaciation termination although considerable redistribution of glacial sediments has occurred by strong Holocene bottom currents (Kenyon, 1986). The sediment distribution down the continental slope is characterized by a progressive increase of the silt and clay content with water depth with a marked increase in fine sediment below 1000 m, although coarse sediments with glacial pebbles are also found at greater depths (Bett, 2001).

Three main water masses occupy the channel. The near-surface Rockall Channel is a conduit for saline waters of southern origin to flow northwards into the Nordic seas (New et al., 2001; New and Smythe-Wright, 2001). The upper one, derived from the north western Atlantic, extends down to about 1500 m and the Labrador Sea Water flowing northwards is found at intermediate depths, between 1600 and 1900 m water depth (e.g., Ellett and Martin, 1973). Deeper down, the denser Norwegian Sea Deep Water flowing southwards is found in the deeper part of the channel (e.g., Ellett et al., 1986; van Aken and Becker, 1996). Elongated sediment drifts and sand/silt contourites have been identified in the lower northern Rockall Channel (Masson et al., 2003) at around 1200 m deep, evidencing the shaping action of bottom currents in this part of the channel. In the southeast part of the channel however, bottom currents flow southwards and no evidence of contourites has been reported. Lonsdale and Hollister (1979) inferred a cyclonic circulation of the bottommost waters in the channel based on the bedform features and reported evidence of erosion on the deepest part of the western slope of the channel. However, their data did not allow for further conclusions on the resuspension mechanisms.

The ROCS experiment followed the same approach as the PROCS experiment conducted at 500–1000 m depth in the confined Faeroe–Shetland Channel but was carried out deeper (2500–3000 m).
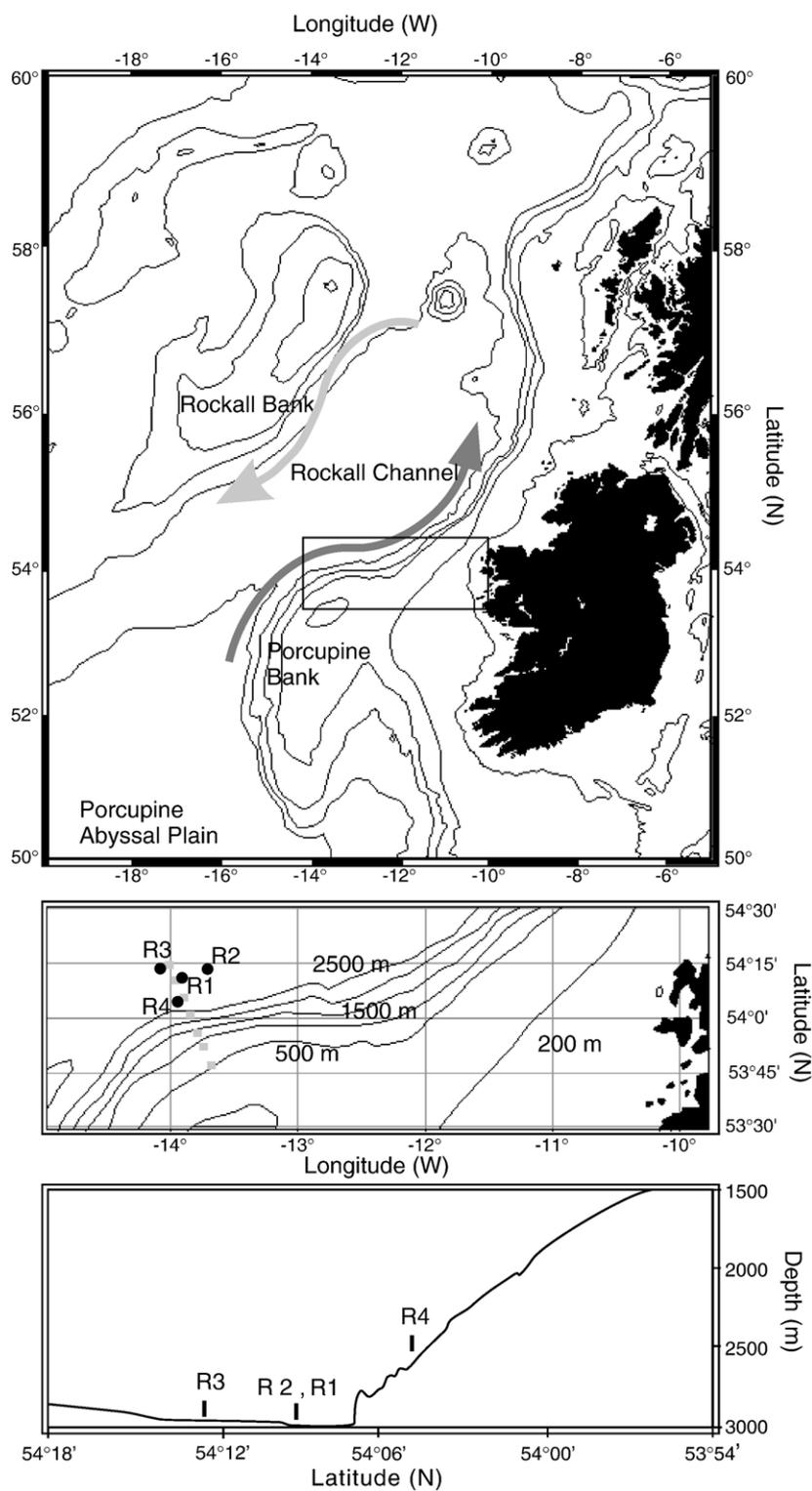
Fig. 1. Map of the study area. Black squares indicate the location of the moorings and the grey circles the position of the CTD stations. Mooring 1 was equipped with an ADCP and a thermistor string and moorings 2, 3, 4 were equipped with near-bottom sediment traps and current meters.

The differences in setting were obvious: a sharp transition from steep slope to flat abyssal plain and weak density stratification versus halfway a continental slope and strong stratification. Nevertheless, at both sites vigorous, short-term and abrupt small-scale ocean processes were observed in a restricted geographical area.

3. Experimental setting, material and methods

A total of 4 moorings were deployed at the foot of the slope of the Rockall Channel for a period of about 6 weeks between 18 July and 31 August 2002. Three moorings (R2, R3 and R4) equipped with 2 sediment traps, 1 optical backscatter sensor (OBS) and 3 current meters each were deployed at 2981, 2969 and 2579 m water depth, respectively. The moorings were deployed in a triangular fashion at mutual distances of approximately 10 km (Fig. 1). An additional Mooring (R1), deployed at 2975 m water depth, was equipped with a fast-sampling upward looking acoustic Doppler current profiler (ADCP) and a high-resolution NIOZ-built thermistor string of which the upper section only functioned well. The traps at 30 and 2 m above bottom (mab) of moorings R2 and R3, respectively, malfunctioned due to a failure of the rotation unit.

3.1. Sediment traps and trap samples treatment

Technicap PPS 4 sediment traps with 12 collecting cups (250 ml) were deployed for this study with their apertures at 2 and 30 mab. They are hereafter referred to as the name of the mooring R2, R3 and R4, followed by the height above the bottom at which they stand (R4-30, R4-2...). All traps collected during 12 successive and synchronised intervals from July 18 0:00 h (day 198) to August 31 24:00 h UTC (day 242). The initial 2 cups sampled for 48 h and the subsequent 10 for a period of 96 h each. To allow sampling in a high-energy environment with the PPS 4 traps, they were extended by a 1.5-m high PVC cylinder with a baffled aperture (10 mm hexagons), with the bottom traps mounted in a bottom frame which also carried the release gears and anchor weight. The resulting total length of the cylindrical traps is 2 m and the collecting area of the trap is 0.042 m^2 yielding an aspect ratio of 8. Mooring configuration and sediment trap samples treatment are detailed in Bonnin et al. (2002), except that the entire sample had to be processed due to the limited amount of collected material and to avoid bias due by sample splitting.

3.2. Trapping efficiency

To assess the efficiency of the sediment trapping, their Reynolds numbers (R_t) were computed using the averaged current speed for every single sample interval measured close to the mouth of the traps. The Reynolds number, $R_t = u \times D / v$ where u is the flow speed at the trap mouth, D is the diameter of the trap and v the cinematic viscosity, is a dimensionless parameter that together with the aspect ratio and the ratio of flow speed to particle settling velocity, is an important property relating to the collection efficiency of a cylindrical sediment trap (Butman et al., 1986). The calculated R_t values ($T = 2.6$ °C, S = 35.05, $v = 1.6 \times 10^{-6}$ $m^{-2}s^{-1}$) varied between 6.6×10^3 and 4.2×10^4 for current speeds of 4.2 and 26.9 cm s^{-1}, respectively. Since the settling velocity is variable and unknown and the aspect ratio is constant, only the Reynolds number can be considered. According to the US-GOFS (1989), the collection efficiency of traps with an aspect ratio >1 is expected to decrease with increasing R_t for a fixed aspect ratio and the ratio of flow speed to particle settling velocity. Gardner et al. (1997) however, showed that the collection efficiency of cylindrical traps did not decrease for trap R_t numbers up to 4.3×10^4 which is higher than the those calculated for our traps. Also, if a noticeable effect of R_t on collection efficiency existed, we should have observed a negative correlation of TMF with R_t. Furthermore, Gardner (1985) observed that cylindrical traps with aspect ratios >5 appropriately sampled the particle flux under moderate flow conditions but still may give biased results under high-flow conditions (Butman, 1986; Butman et al., 1986; Gust et al., 1994). For identically configured sediment trap moorings in the Faeroe–Shetland Channel where near-bottom current speed often exceeded 60 cm s^{-1}, Bonnin et al. (2002) showed that the traps experienced little tilt and that their overall trapping efficiency was satisfactory. In the present study however, current velocity never exceeded 35 cm s^{-1} and tilt angles measured by sensors mounted on each trap body never exceeded a few degrees.

For the different reasons listed above, we conclude that our trap data are not strongly biased by varying flow speed or trap tilt. Based on laboratory flume experiments, Gust et al. (1996) developed a particle accumulation model to correct for the effect of flow and particle size on collection efficiency and derived real in-situ fluxes from trap measurements. However, such correction requires that many parameters such as trap yield, advective and gravitational particle entry area, sinking-particle concentration, and settling veloc-

ity are known. Collectively, such controls are as yet beyond direct measurement by modern techniques and therefore do not allow to the precision of our trap data, although error propagation suggests they are accurate within 10% of the total mass flux estimates. Furthermore, we are aware that the mass fluxes we recorded included both gravitational and advective components but since the goal of this study is to assess the resuspension processes near the bottom rather than establish a quantitative budget of particles reaching the bottom, the input of sea bed material is not considered a bias.

3.3. Surface sediments and particle analysis

Surface sediments were sampled using a multicorer (Barnett et al., 1984) that recovered virtually undisturbed sediment with a thickness up to 30–40 cm at 3 locations on the slope at depths of 1988, 2695 and 2981 m. Core tops were freeze-dried prior to grain size analysis using a Coulter LS230 laser particle-sizer (Konert and Vandenberghe, 1997). Approximately 500 mg of freeze-dried material was suspended in ~20 ml de-ionised water and placed in ultra-sonic
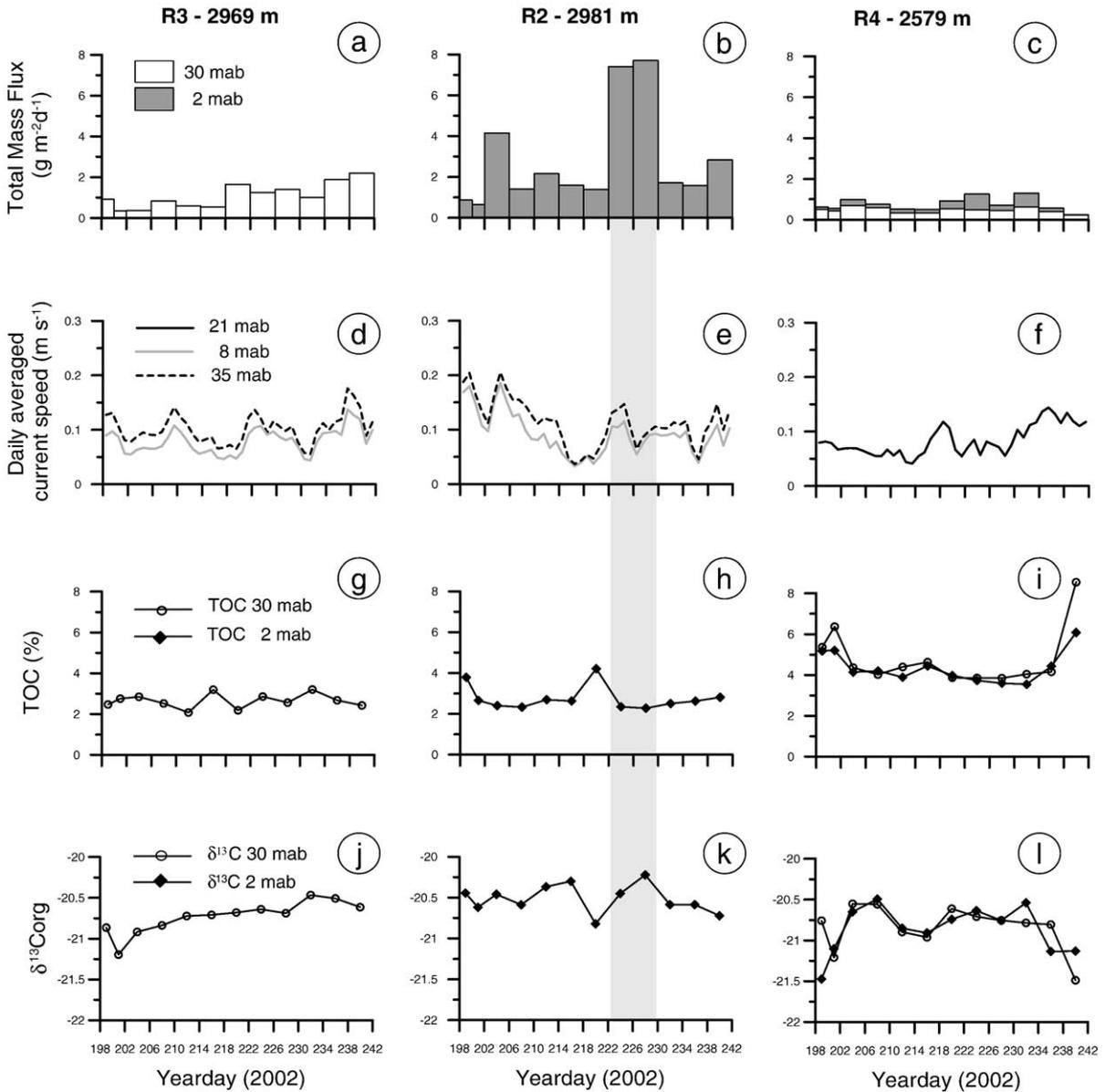

Fig. 2. TMF (a–c), Daily averaged current speed (d–f), C_{org} (g–i) and $\delta^{13}C_{org}$ (j–l) for trap material intercepted at 2969, 2981 and 2579 m. The shaded band indicates the interval of maximum resuspension at 2981 m.

Table 1
Depth and location of surface sediment samples with indication of the
C_{org} content and $\delta^{13}C_{org}$ of the core tops

Station	Depth (m)	Latitude (N)	Longitude (W)	TOC (%)	$\delta^{13}C$
15	2981	54.15388	− 14.07368	0.217	− 21.085
16	2695	54.09288	− 14.03863	0.272	− 21.105
17	1988	54.02560	− 13.99313	0.410	− 20.336

bath for ~5 min. The suspension was sieved over 1 mm and ultra-sonicated internally. Grain size distributions were corrected for the weight retained on the 1 mm sieve. A similar method was used for particle size analysis of the trap samples (when sufficient material was available), using ~200 mg of freeze-dried material.

Freeze-dried sediment trap and core top samples were pulverised in an agate mortar and analysed with a Flash EA 1112 Elemental Analyser interfaced with a Finnigan MAT 252 mass spectrometer to determine the stable isotope composition ($\delta^{13}C_{org}$) and organic carbon content (C_{org}). Between 200 and 800 μg of material (~100 μg of organic carbon) was weighed in a silver cup. Inorganic carbon was removed by progressive and controlled acidification with 1 N HCl. Isotope values were calibrated to a benzoic acid standard ($\delta^{13}C = -27.8‰$ with respect to PDB) and corrected for blank contribution.

3.4. Current meters and optical backscatter sensors

Moorings R2, R3 and R4 were equipped with current meters positioned at 8, 21 and 35 mab. Aanderaa RCM-8 current meters (21, 35 mab) and RCM-11 current meters (8 mab) all included temperature sensors and sampled once every 2 min. Mooring R1 was a bottom lander containing an upward looking 300 kHz ADCP and the NIOZ-built thermistor string (van Haren

et al., 2001). The instruments sampled with a high temporal (15 and 30 s, respectively) and spatial resolution (1 m) between 2 and 82 mab for the temperature, the 3 components of the current velocity, and the echo amplitude (acoustic backscatter strength). Current velocities were positive down-slope for the cross-slope component and positive to the northeast for the along-slope component.

Seapoint turbidity meters (OBS) sampling every 12 min were mounted on the sediment traps to measure the infrared light (wave length 880 nm) backscattered by particles at angles between 15° and 150°. Optical sensors are mainly sensitive to particles finer than 20 μm (Bunt et al., 1999) and hence are insensitive to larger particles such as phytodetritus aggregates or coarse sediment particles. Because of the difficulty to calibrate such data and the potential bias due to inadequate calibration, turbidity values are given in their output unit, i.e. Volt as measured by the OBS. In addition to the OBS mounted on the traps, a similar OBS was mounted on a Seabird 911 CTD frame that was deployed at several stations on a transect across the south-east slope of the Rockall Channel (Fig. 1).

4. Results

4.1. Total mass flux

Microscopic observations revealed that the particulate matter collected in all the traps consisted essentially of fluffy material composed of filaments, mucus and aggregates (reaching several mm in size) and faecal pellets, with few planktonic foraminifera and rare silt-sized grains. The total mass flux (TMF) for each trap is given in Fig. 2(a–c). Time series of particulate fluxes at all three locations displayed different patterns with no
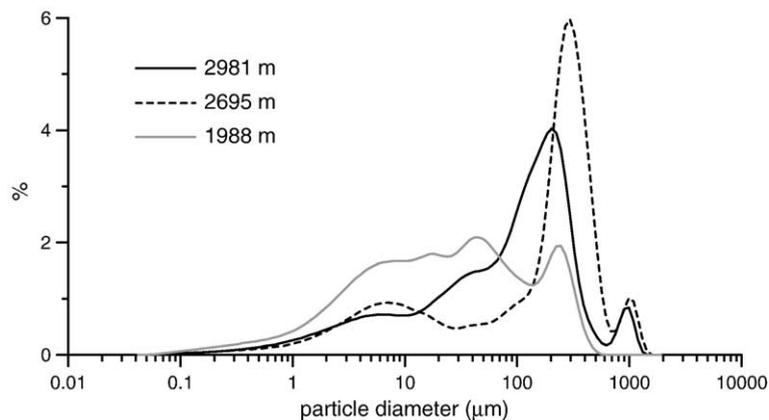

Fig. 3. Grain size spectra of surface sediments at 1988, 2695 and 2981 m water depth.

Table 2
Water depths, current meter types, height above the bottom, averaged along-slope and cross-slope velocities for the whole deployment period for moorings R2, R3 and R4

Mooring	Water depth (m)	Instrument	Height above bed (mab)	$\langle u \rangle$ (cm s^{-1})	$\langle v \rangle$ (cm s^{-1})
R2	2981	RCM-11	8	4.1	−0.3
		RCM-8	35	5.9	0.3
R3	2969	RCM-11	8	−1.1	−0.9
		RCM-8	35	−1.7	−0.4
R4	2575	RCM-8	21	−2.4	0.9

obvious common event which indicate that the conditions prevailing for particle resuspension and transport were different from one station to another despite their proximity. TMF was higher at the foot of the slope (R2)

and slightly off the slope (R3) than higher up (R4). Data from mooring R4 indicate that the TMF at 2 mab (0.7 g m^2 d^{-1}) was on average higher by about a factor 2 compared to the flux at 30 mab (0.4 g m^2 d^{-1})
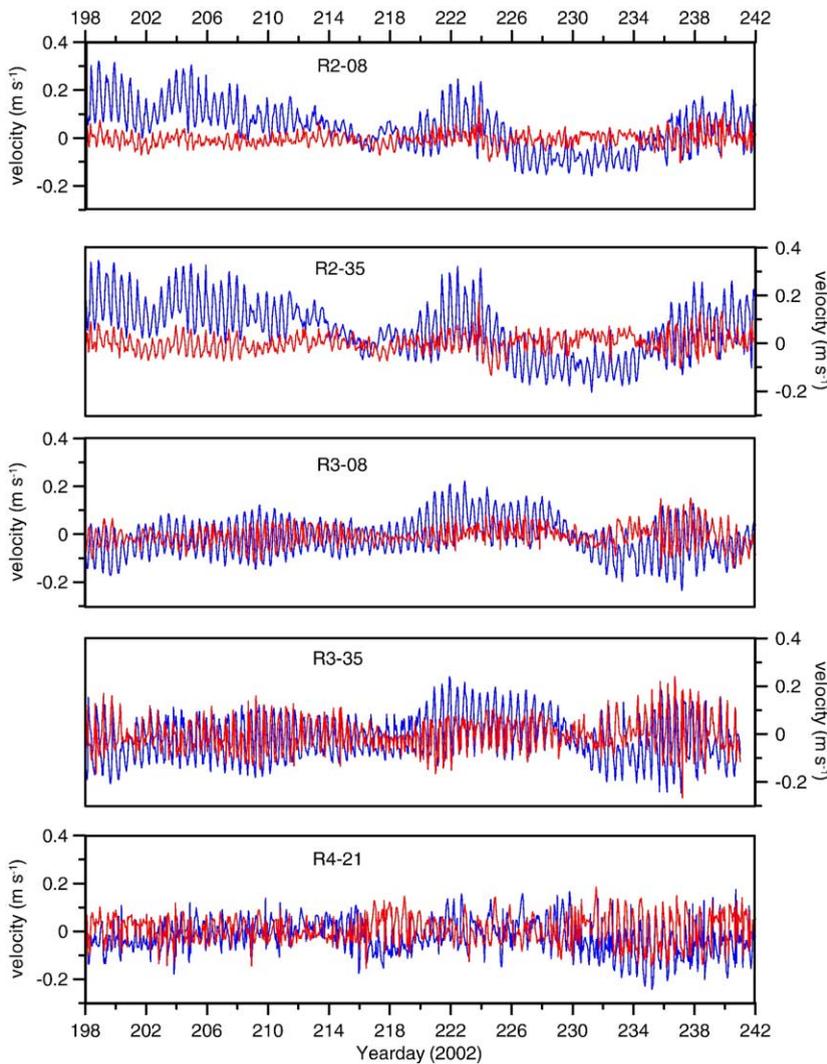

Fig. 4. Along-slope (blue) and cross-slope (red) components of the current velocity at 8 and 35 mab (for moorings R2 and R3) and at 21 mab for mooring R4. The cross-slope is positive down-slope and the along-slope positive to the northeast. (For interpretation of the references to colour in this figure legend, the reader is referred to the web version of this article.)

throughout the deployment period, clearly suggesting a secondary input of bottom-derived material. During the periods of weakest near-bottom current speed a minimum background flux of 300 mg m^2 d^{-1} was observed in all traps. While no major event were observed in traps R4 and R3, trap R2-2 displayed a large TMF increase between days 222 and 230 with TMF reaching 7.7 g m^{-2} d^{-1} and a somehow smaller increase (4.1 g m^{-2} d^{-1}) between days 202 and 206.

4.2. C_{org} and $\delta^{13}C$ of resuspended particles

The C_{org} content of sediment trap samples ranged between 2% and 8.4% with a higher content for samples with lower TMF although no linear relation emerged (Fig. 2g–i). From R4 traps, C_{org} was measured both at 2 and 30 mab but except for the last interval, no clear difference was observed between those two heights. However a significant difference in the C_{org} was observed between the shallower station, where C_{org} was constantly in excess of 3.5%, and the deeper stations where C_{org} was always below 3.5% except between days 218 and 222 (R2-2). The high C_{org} content between days 218 and 222 corresponds to a low

flux period that preceded the maximum flux event (Fig. 2b and h).

Carbon stable isotope values ranged between −20.2‰ and −21.4‰ with the lowest value corresponding to the lowest TMF and vice versa (Fig. 2j–l). With increasing agei of the organic matter, the $\delta^{13}C_{org}$ will become isotopically heavier as ^{12}C is preferentially remineralised, indicating that the lower $\delta^{13}C_{org}$ reflected a higher input of fresher organic material. On average, the $\delta^{13}C_{org}$ was lower from traps R4-30 and R-2 and increased with increasing water depth. The $\delta^{13}C_{org}$ signal in R4-30 and R4-2 showed a similar trends and values. For R3-30, the $\delta^{13}C$ increased progressively with increasing TMF while for R2-2, $\delta^{13}C_{org}$ values remained constant except for the relative abrupt drop between days 218-222. The fairly homogenous $\delta^{13}C_{org}$ in all traps indicates that material intercepted by the traps at all depths is not significantly different in composition. The relatively high C_{org} content together with the microscopic observation of the samples suggests that this material is essentially composed of a "rebound" mixture of refractory sediment particles and fresh labile phytodetritus and aggregates that had already been in contact with the seabed sensu
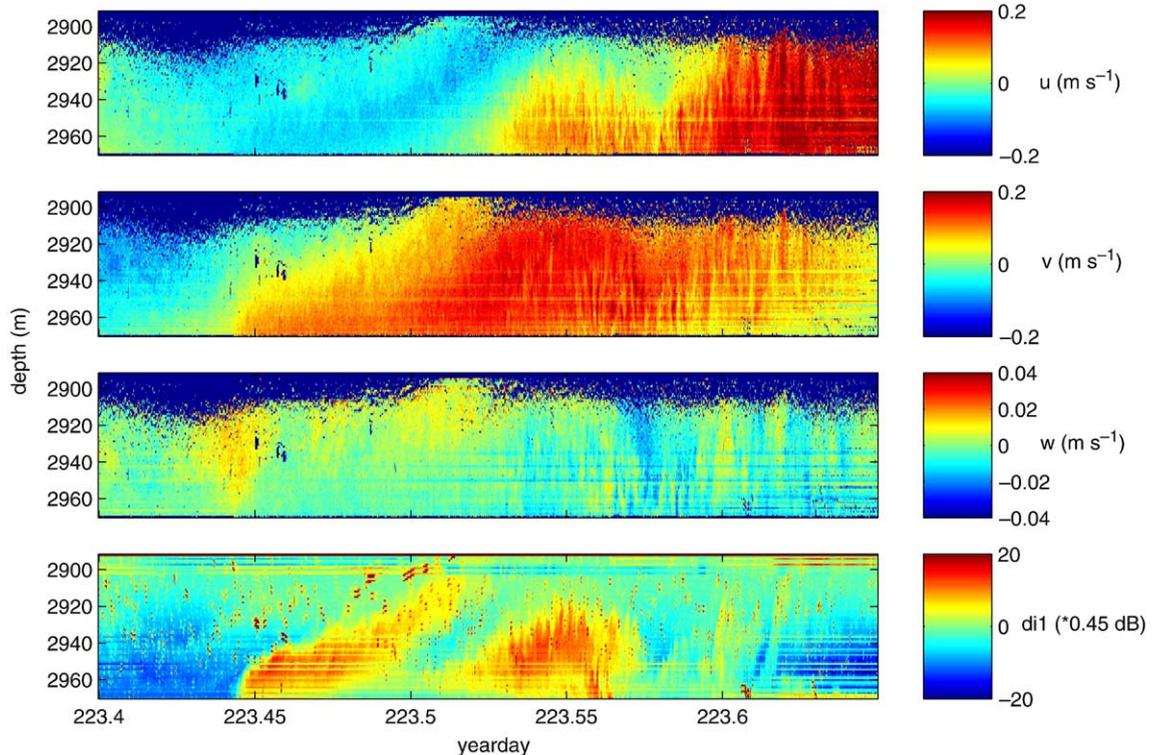

Fig. 5. *u* (along-slope, positive to the northeast), *v* (across-slope, positive down-slope) and *w* (vertical, positive upward) components of the current velocity and echo intensity (lowest panel) measured by the ADCP mounted on mooring R1. The time window is 6 h and data show a burst in *u*, *v* and echo intensity centred on 223.5.

Walsh et al. (1988). Furthermore, $\delta^{13}C_{org}$ values of trap material and surface sediments are close and hence indicate that resuspended seabed particles were the main source of the intercepted material (Fig. 2j–l, Table 1).

4.3. Surface sediments

Sediments show a clear depth zonation. At 2981 m an upper light brown layer about 6 cm thick covered greyish silty sediments. The core top consisted of bivalve shells and small sponges with a thin layer of fluff. At 2695 m the multicorer did not penetrate deeper than 6 cm due to the presence of abundant glacial pebbles and cobbles embedded in light brown sandy sediments about 2 cm thick overlaying clayish material. At 1988 m, the surface sediments essentially consisted of light brown muddy sand observed throughout the core and covered with a thin fluffy layer. The grain size of core tops (Fig. 3) varied with depth, with coarser particles at 2695 m and finer ones at 1988 m. The median grain size was about 35 μm at 1988 m, 220 μm at 2695 m and 100 μm at 2981 m. Grain size spectra of surface sediments from 2981 m were similar to the one at 2695 m

with a distribution marked by 2 peaks at ~1000 and ~200 μm but with a lower content of coarse particles. At 1988 m, grain size showed a different and less distinct distribution without the mode ~1000 μm and dominated by particles finer than 60 μm.

In the core tops the Corg content ranged from 0.41% at 1988 m to 0.21% at 2981 m and the $\delta^{13}C_{org}$ from $-20.33‰$ to $-21.10‰$ at 2695 m, respectively (Table 1). Both C_{org} and $\delta^{13}C_{org}$ were higher at 1988 m than deeper down and suggest a higher contribution by fresh organic material at that depth. At 2695 and 2981 m, the C_{org} content and $\delta^{13}C_{org}$ were similar and indicated no major difference in organic matter input in the deeper part of the channel.

4.4. Variability of near-bottom current velocity

Average current velocities over the whole observation period showed an along-slope component orientated poleward at mooring R2 (both at 8 and 35 mab) but orientated equatorward at moorings R3 and R4 (Table 2). For the cross-slope component, averages were always low (<1 cm s^{-1}) without any clear trend. Hourly averaged current velocity components
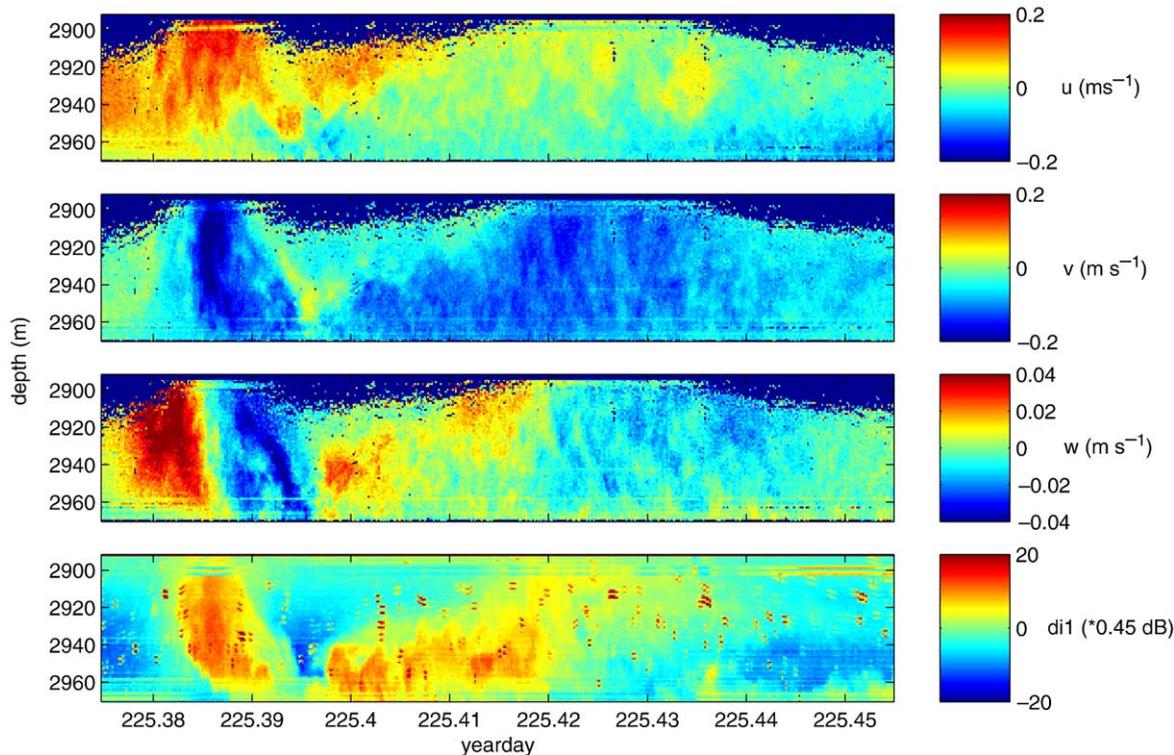

Fig. 6. u (along-slope), v (across-slope) and w (vertical) components of the current velocity and echo intensity (lowest panel) measured by the ADCP mounted on mooring R1 (signage similar to Fig. 5). The time window is 2 h and data show a burst in u, v, w and echo intensity centred on 225.4.

(along and across-slope) showed distinct tidal variations of semidiurnal frequency at R2 and R3, and a more noisy signal at R4 (Fig. 4). Current velocity is generally higher at 35 mab than at 8 mab. The maximum along-slope velocity (34.7 cm s^{-1}; poleward) was observed at 35 mab on R2 water depth and the maximum cross slope velocity (26.7 cm s^{-1}; up-slope) was observed at 35 mab on R3.

A noticeable feature was observed from mooring R2, where an abrupt increase in the cross-slope component oriented down-slope occurred on day 223 reaching 13.7 and 17.2 cm s^{-1} at 35 and 8 mab,

respectively. This sudden down-slope peak was also clearly observed in the ADCP data (Fig. 5) which show that this event is accompanied by elevated backscatter. Since stratification, in particular thermal stratification, at the base of the slope is weak, acoustic backscatter produced by turbulence is very unlikely (Thorpe and Brubaker, 1983) therefore implying that the backscatter signal from the ADCP is mainly due to suspended material. Change in grain size could also be responsible for such increase in the echo intensity. However, acoustic devices are more sensitive to relatively large particles (>20 μm, Lynch et al., 1994)
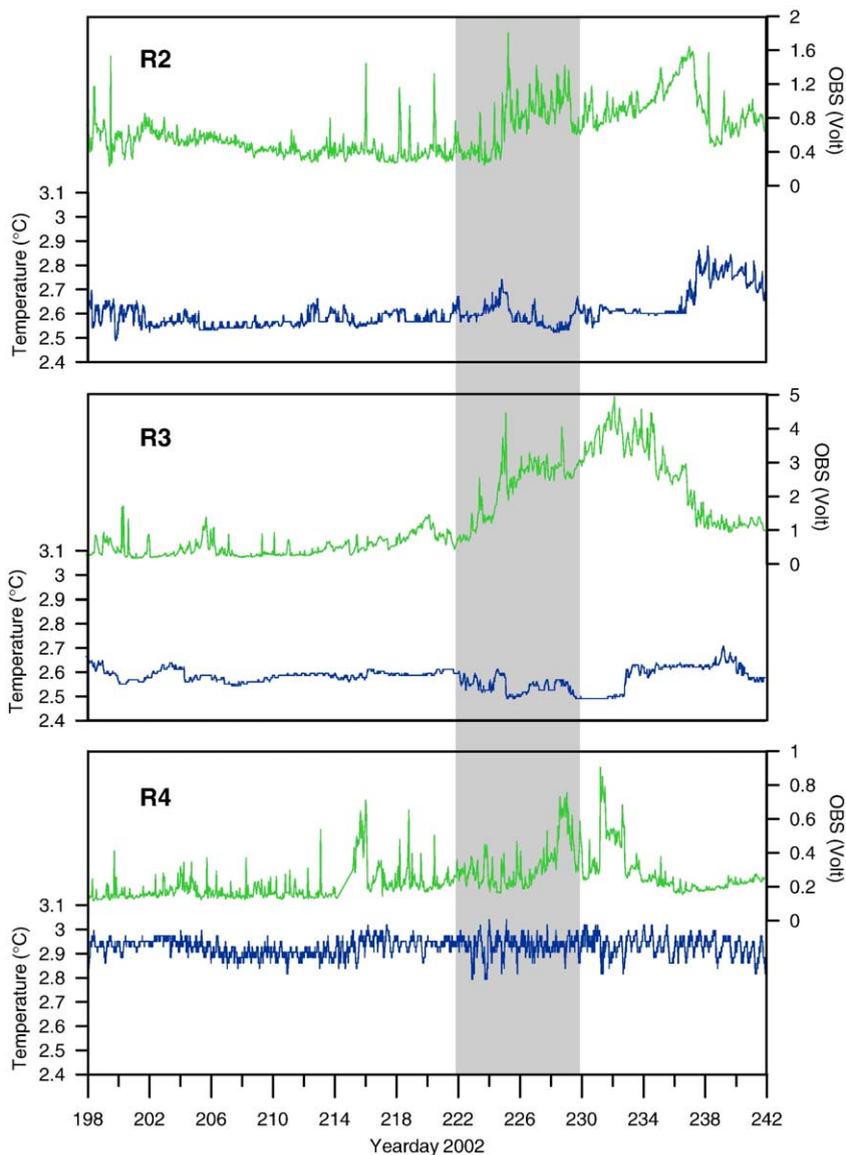

Fig. 7. Turbidity from the OBS mounted on bottom traps (2 mab) and temperature records from current meters (8 mab) for the 3 stations. The shaded area indicates the interval of maximum total mass flux as shown in Fig. 2.
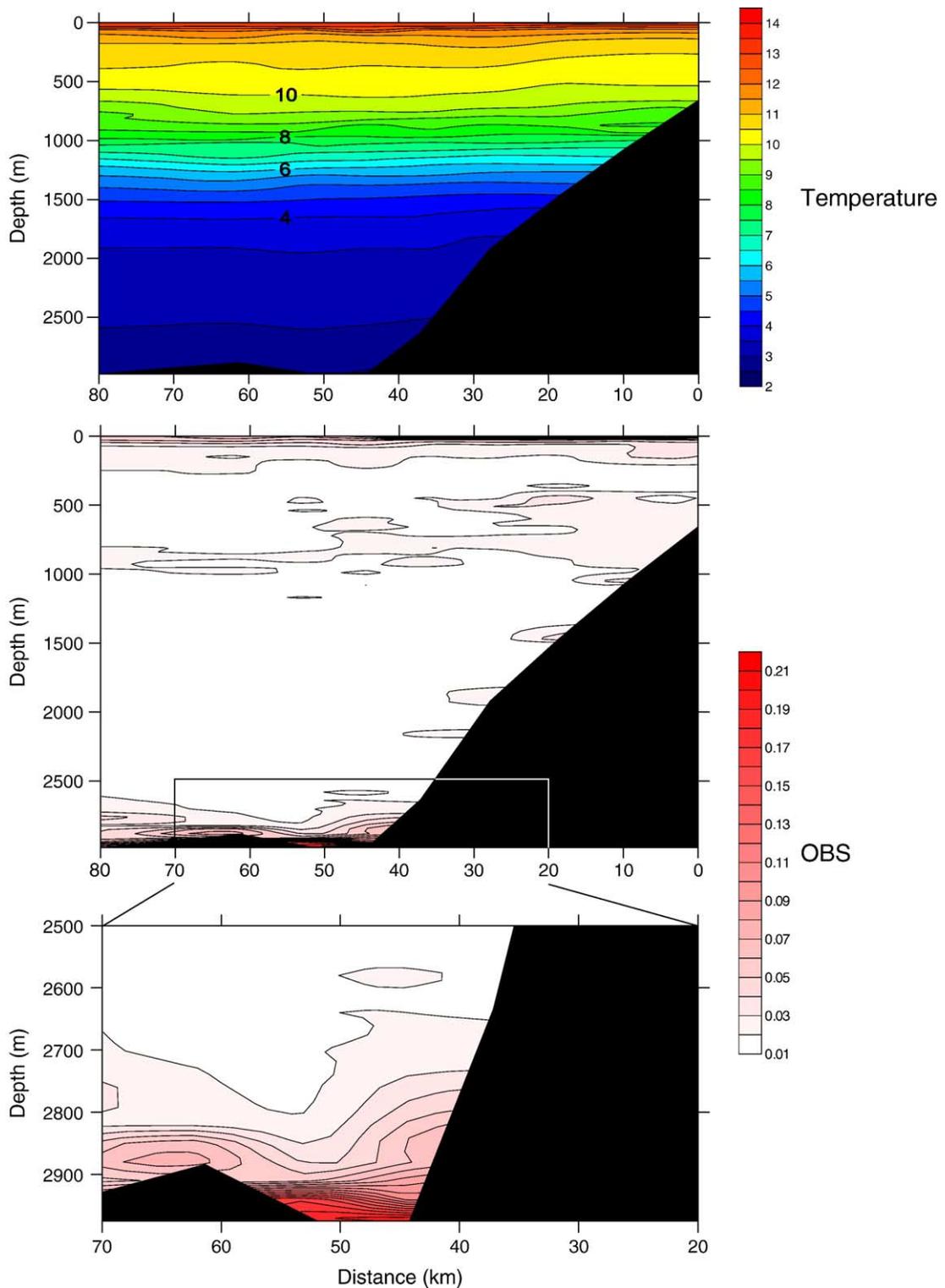
Fig. 8. Profile of temperature (°C) and turbidity (Volt) from the CTD stations across the Rockall Channel as shown in Fig. 1. The lower panel is a blow up of the turbidity at the foot of the slope. Note the upslope shape of the turbidity layers.

which rule out the possibility that the increase in the backscatter signal is the response of break-up of aggregates rather than increase of concentration of particles. Furthermore, trap R2 does indicate any increase in the mass flux which also support the idea of resuspension. Another burst in current velocity was observed on day 225 by the ADCP (Fig. 6). It lasted for about 10 min, reached 80 mab and was accompanied by a burst of elevated echo intensity, similar to the day 223 event. However, in contrast to the previous event, the cross-slope component was mainly orientated up-slope, and both the along-slope and vertical component were fairly high. This abrupt increase in both current speed and turbidity near the bottom corresponded to the time of maximum TMF calculated from R2-2 (Fig. 2b) and further indicated that the particles intercepted during this interval originated from resuspended seabed material. It is noted that the abrupt current changes occur over a period of about 4 days having a tidal periodicity, but at slack water when the main tidal current speed is negligible.

4.5. Physical properties of the near-bottom water

Temperature near the sediment traps as recorded by the temperature sensor of the current meters at 8 mab (for moorings R2 and R3) and at 21 mab (for R4) was fairly constant over the whole recording period, ranging from 2.4 to 2.9 °C at R2 (Fig. 7) and R3 and between 2.75 and 3.05 °C at R4. A drop of 0.2 °C following a more progressive increase was measured at 2981 m on day 225 and was concomitant with the increased turbidity at 2 mab. A similar turbidity peak was also observed from R3 but not from R4. Another large increase in temperature of about 0.3 °C was measured on day 237 at R2 only, related to a moderate increase in the current velocity and to a drop of the near-bottom turbidity (Fig. 7). In general, turbidity data do not correlate well with TMF. Although a higher turbidity was measured at R3 than at R2, less material was intercepted by the trap. This may be due to the higher position above bottom of the trap R3-30 compared to R2-2. Furthermore, for mooring R2 a period of elevated turbidity around day 236 did not correspond to a higher particle flux (Fig. 3) nor to a higher near-bottom current velocity (Fig. 4). CTD profiling showed that the strongest temperature gradient is found around 1000–1200 m while the highest suspended particle concentration was observed at the foot of the slope and was fairly low higher up on the slope (Fig. 8). Turbidity was higher at the foot of the slope than higher up, consistent with the presence of finer sediment at the deeper site and to the

lower turbidity shown by the moored OBS at that depth (Fig. 7).

5. Discussion

5.1. Strong variability of the fluxes

High temporal variability of TMF was observed in almost all the traps. If low TMF occurred during low averaged current speed, higher TMF was not always observed at higher current speed (Fig. 2a–f). Large flux intervals (202–206, 222–226 for R2-2 and 234-242 for R3-30 to a lesser extent) are concomitant with increased near-bottom current speed. The largest trap flux however did occur when current speed and along-slope and cross-slope velocity components were low.

Microscopic observations revealed that the material intercepted in the traps deployed in the Rockall Channel consisted mainly of loose phytodetritus and aggregates that are easily resuspended. Further examination of the data revealed that the Rockall Channel traps samples have a higher C_{org} content than in the FSC (Bonnin et al., 2002), even during high fluxes, and confirm that resuspended material at the foot of the slope of the Rockall Channel is, on average, less refractory than what was resuspended in the FSC. This might be due to the large amount of coarse lithogenic particles intercepted during the PROCS experiment. Pulsed input of phytodetritus to the seabed following blooms can also explain the presence of relatively fresh material on the abyssal plain, as Lampitt (1985) found in the nearby Porcupine Abyssal Plain and Beaulieu and Smith (1998) in the abyssal NE Pacific. The TMF measured in this study are higher than the particle flux measured in the deep (4600 m) abyssal hill province of the northeastern Atlantic (Auffret et al., 1994). However they are small compared to those observed on the south-east slope of the FSC (Bonnin et al., 2002, 2005) where considerable resuspension fluxes were measured at 700–800 m water depth and much lower at the foot of the slope. Indeed TMF with a high proportion of coarse sediments reached 350 g m^{-2} d^{-1} at 800 m which is two orders of magnitude higher than in the Rockall Channel. Coarse particles (benthic forams, quartz and feldspar grains) as observed in the traps deployed in the FSC were not found here. However, given the short distance between the traps and the expected quiet conditions, the differences observed in the Rockall Channel in the TMF and the near-bottom current regime remain significantly large. Moreover, the lack of correlation in the TMF, partic-
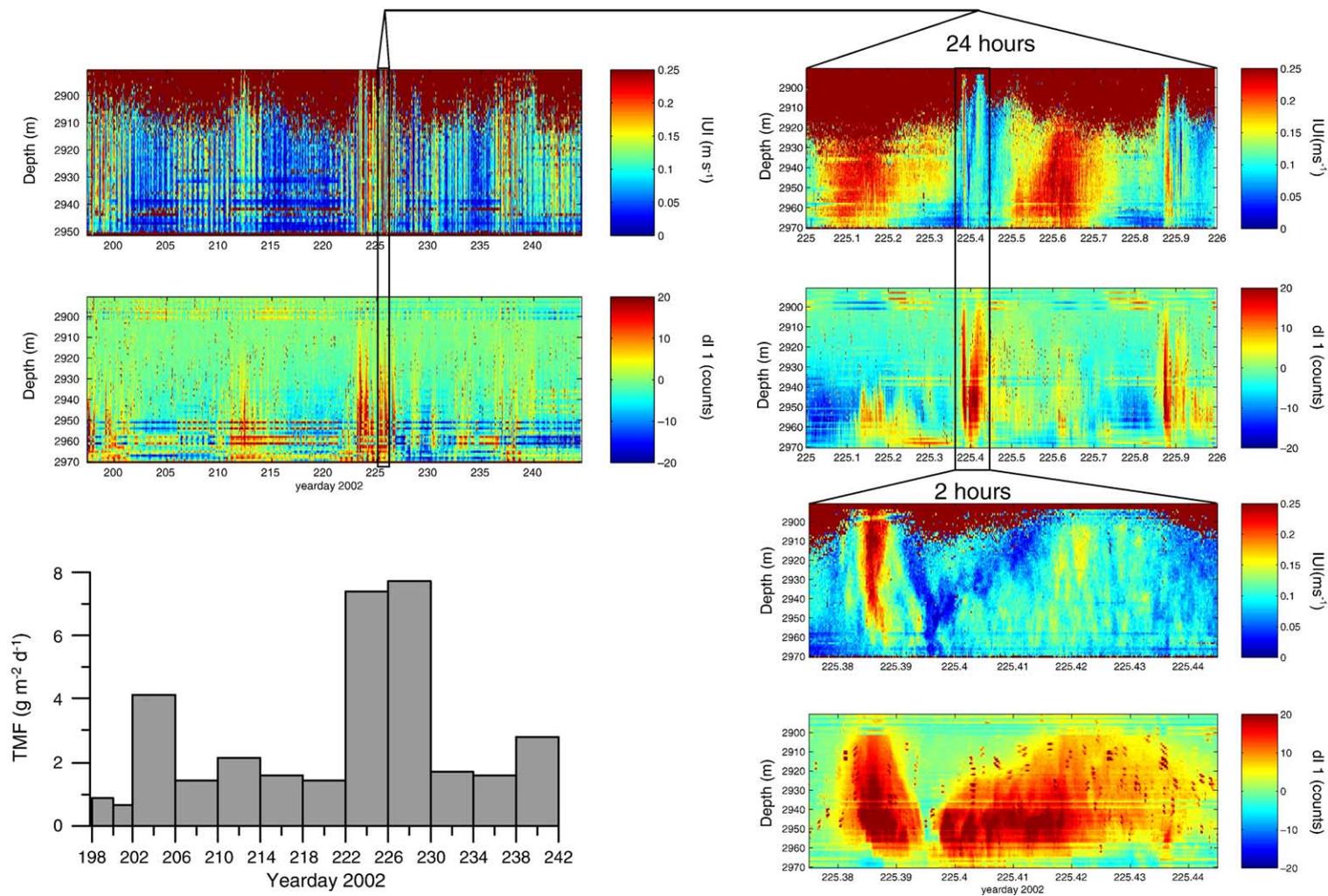
Fig. 9. Current speed and turbidity (echo sounder) measured by the ADCP deployed at R1 site (2975 m) during the 6 weeks of the deployment. Results from R2-2 (2981 m) show the correlation of the highest TMF with the sudden burst in the current speed on day 225 and the corresponding increase in the near-bottom turbidity.

Table 3
Comparison of observations from PROCS (Faeroe-Shetland Channel) and ROCS (Rockall Channel)

Differences		Similarities
PROCS	ROCS	PROCS–ROCS
500–1000 m deep Sloping bottom	2500–3000 m deep Changing topography	High TMF spatial and temporal variability
Averaged current speed ~25 cm s^{-1}	Averaged current speed ~10 cm s^{-1}	Background resuspension flux associated to averaged current speed
Coarse and refractory material (sand) resuspended during highest TMF	Only phytodetritus and fluffy material resuspended during highest TMF	Abrupt changes in the current speed (bursts)
Maximum TMF: 350 g m^{-2} d^{-1}	Maximum TMF: 8 g m^{-2} d^{-1}	Maximum TMF associated to bursts
No tidal periodicity	Tidal periodicity	Temperature drop accompanying burst and increase in TMF

ularly between traps R2 and R3 located at similar depths, suggests the importance of localised processes in facilitating resuspension of seabed material. This agrees with the observations of Lampitt et al. (2000) who concluded from a trap experiment in the Porcupine abyssal plain that changes in the suspended load near the bottom was probably due to variations in the current speed or direction rather than scavenging by primary flux particles.

5.2. Hydrodynamics and resuspension potential

Resuspension of bottom material is very much linked with current velocity. Lampitt (1985) estimated from a study in the Porcupine Abyssal Plain in the north Atlantic that near-bottom currents of ~7 cm s^{-1} should be sufficient to resuspend loose phytodetritus flocks freshly deposited on the seabed. Furthermore, from studies conducted in the deep Rockall Channel at a site just a few miles west of our study area, Thomsen and Gust (2000) concluded that a flow speed at 1 mab of 9 to 23 cm s^{-1} was sufficient to resuspend the loose phytodetritus aggregates deposited on the sea bed. However, a current speed >45 cm s^{-1} was required to initiate transport of the underlying sediment, hence proposing a two layer concept for the water-sediment interface. Since current speeds never exceeded 35 cm s^{-1} during our observation period, this suggests that only aggregates are resuspended rather than the underlying sediment which is in good agreement with the lack of coarse sedimentary particles intercepted by our traps.

From the data obtained during the ROCS study it appears that sediment resuspension is not only related to an increase in near-bottom current velocity, as highest TMF (between days 222–230 for mooring R2) was measured during intervals of relatively low current speed (Fig. 2). Hence, absolute current speeds alone cannot account for the temporal variation in the TMF (Fig. 2b and e) and a different mechanism independent

of flow speed is needed to explain the higher fluxes. Settling of primary material is unlikely to explain this elevated flux near the bottom as 1) the C$_{org}$ content of the material intercepted during the flux increase is not higher, hence not reflecting higher supply of organic matter and 2) in case of increased settling of surface material it would be difficult to explain why only one trap recorded the flux increase while other traps located few miles apart did not do so. Indeed, the observation that elevated fluxes were only found in one of the traps, implies a localised hydrodynamic mechanism which has a comparatively small spatial scale as compared to, for example, a boundary current which may elevate bed shear stresses (and thus resuspension) over a wide region. Furthermore, the burst in the cross-slope velocity, backscatter and particle mass flux on day 225 occurred when the along-slope (tidal) current speed was low, suggesting that lateral advection is unlikely. Also, the echo intensity was strongest at the sea bed and decreased upwards which is suggestive of sediment being resuspended from the local bed rather than lateral advection of material from a remote source. Furthermore, the abruptness of the increase in both current velocity and acoustic backscatter together with the short duration of the events and the low mean along-slope currents strongly suggest local resuspension due to short but intense hydrodynamic processes.

Bonnin et al. (2005) showed that resuspension of coarse material in the FSC was closely related to abrupt changes in the near-bottom hydrodynamics. Such abrupt changes in the near-bottom hydrodynamics also appear to be at the origin of the resuspension of surface layer aggregates observed in the Rockall Channel (Fig. 9). A comparative table of both ROCS and PROCS result is presented in Table 3. Resuspension fluxes were highly variable in space and time with resuspension of loose aggregates and phytodetritus occurring at all times related to fluctuation of the current speed, while intense resuspension appeared to

be associated with abrupt changes of the near-bottom hydrodynamics. Despite those similarities between the two areas, some important differences exist as no massive resuspension of coarse and refractory sediment (such as quartz sand) was observed in the Rockall Channel whereas it constituted up to 70% of the resuspended material in the FSC (Bonnin et al., 2002). Furthermore, resuspension in the Rockall Channel had a tidal periodicity with current bursts occurring at slack waters while in the FSC no tidal frequency was observed. Maximum near-bottom turbidity and resuspension in the FSC was found at mid-slope depth where the major pycnocline impinged. In the Rockall Channel this maximum is found at the foot of the slope, far below the pycnocline (Fig. 8). Hence, the mechanism facilitating resuspension at the base of the slope of the Rockall Channel seems not related to the pycnocline impinging on the slope, but rather to stratification in general thereby affecting motions over the entire slope and adjacent abyssal region.

5.3. Resuspension mechanism

From observations made over the slope of the Faeroe–Shetland Channel (FSC), Hosegood et al. (2004) and Hosegood and van Haren (2004) argued that bursts in the current speed associated with strong waves of elevation created strong up-slope water surges accompanied by turbulent conditions at the seabed that facilitated the large resuspension fluxes. The identified phenomenon was referred to as a solibore which may take the form of either a dispersive wave train of internal solitary waves (ISW) or of a series of highly turbulent boluses travelling along and across the slope. The resuspension of sediment was further related to the formation of a "rotor" at the leading edge of the wave train characterised by strong upwards velocity (up to 16 cm s^{-1}) immediately followed by a downwards return flow. Such a mechanism has been also shown in a laboratory study on sediment resuspension where 10% to 75% of the incident wave energy appeared lost to dissipation and mixing (Boegman et al., 2005). The cloud of suspended material emanating from the echo-intensity on day 225 compared well with the structure expected from a solibore with a rotor at the front resulting from the convergence at the leading edge and a downward return flow followed by a longer relatively smooth tail within which the sediment is constrained, similar to the ISW train of event S2 in Hosegood and van Haren (2004). From a dynamical perspective, the characteristics of the solibore observed here are similar to what was observed in the FSC as OBS contours at

the foot of the slope show some upslope motion near the bottom (Fig. 8). In addition, on day 225 at R2, a drop in temperature was recorded just before the turbidity and TMF increased, comparable to what was recorded in the FSC prior to the major resuspension event. However, given the absence of the slope at the location of mooring R2 (mooring R2 is located on a flat bottom at the base of the slope, Fig. 1), the mechanism generating them appears to be different.

The results from the ADCP on R1 (Fig. 9), showed that bursts in the velocity occurred on several occasions with 2 markedly strong events observed on day 225 occurring within a few minutes only and associated with the highest TMF of R2-2. Near-bottom turbidity (Fig. 9) showed a slight increase during maximum current speed (225.1–225.2 days) but a much more abrupt and intense turbidity increase during slack waters (225.4 days and 225.9). Furthermore, during this period of maximum turbidity, the ADCP was able to measure current velocity up to 80 mab while it was limited to 60 m at other times probably due to the lack of suspended material above this depth. This indicates that the burst in current speed at that moment was sufficiently energetic to bring particles in suspension to 80 mab. In order to calculate the theoretical height (h) of the benthic boundary layer, Beaulieu and Baldwin (1998) used the following equation for the steady, turbulent Ekman layer:

$$h = \kappa u_* / f$$

where κ is the von Karman's constant (approximately 0.4), f is the Coriolis parameter and u_* the critical shear velocity. We applied the same equation with $f = 1.18 \ 10^{-4} \ s^{-1}$ at our study site and used the u_* values (0.6 to 1.6 cm s^{-1}) given by Thomsen and Gust (2000) from direct measurements in the Rockall Channel at similar depths (2820 m). We obtain values for h between 20 and 54 m which is considerably lower than the 80 m observed during the burst in echo intensity therefore suggesting local generation of the observed turbidity.

The rotors accompanying the solibores and their ability to resuspend sedimentary particles are things that we observed and that are responsible to for sediment transport to a greater degree than high-bed shear stress alone — i.e. it's the nature of the flow (with a non-negligible vertical component) rather than its magnitude alone that determines their ability to resuspend material. As was already advanced by Beaulieu and Baldwin (1998), such local resuspension may have occurred in response to intermittent "bursts and sweeps" which they attributed by the averaging of the

current speed, although no observation of sufficiently strong current was made. Here we illustrate from the ADCP data what those "bursts and sweeps" would look like at those depths.

Data from the event that occurred on day 223, strongly suggest that other short-term mechanisms may also facilitate sediment resuspension on the deep slope. Interestingly, turbidity during this event, again, is not correlated with the maximum along-slope current velocity that was recorded a few hours later. In the case of this event, no rotor was observed from the ADCP data and furthermore, the flow at times of maximum echo intensity is strongly down-slope which is not compatible with the bore associated with the rotor. At this point, we however have no robust explanation for such increase and we can only speculate. Auffret et al. (1994) and Oey (1998) from studies in nearby areas (Porcupine Abyssal Plain and Faeroe–Shetland Channel, respectively) have described the potential of passing mesoscale eddies to facilitate sediment resuspension even at great depths. For this study, although the eventuality of resuspension induced by a passing eddy cannot be completely ruled out, we believe this to be rather unlikely. In case of a passing mesoscale eddy it would be difficult to explain resuspension at one site only and not at the other 2 located only a few miles apart. Furthermore, analysis of the current data showed no evidence of an eddy at this site. A more likely mechanism could be the occurrence of a gravity current. It has been proposed for the Bay of Biscay that internal gravity waves can propagate highly obliquely on the slope, thereby pushing heavy water up the slope from light water and creating unstable stratification that results in a down-slope flow (Gemmrich and van Haren, 2001). Internal waves can have strongly varying directions and an occasionally obliquely propagating wave is therefore a likely candidate. A landslide that would generate a down-slope gravity current may also be a good potential candidate and could explain the elevated mass flux at that time as well. However, such land-slide would be restricted to the lowermost part of the slope as no evidence of it has been found from the mooring R4 deployed at 2579 m.

6. Conclusions

This study, conducted at the foot of the slope of the Rockall Channel, combined sediment traps deployed at 2 and 30 m above the sea bed with near-bottom current meters and an ACDP sampling at a high rate. Together with the results from an earlier study in the Faeroe–Shetland Channel, they highlight the importance of short-term but intense processes for resuspension of fluff material and the underlying sediments in various slope environments. In particular our results show the potential of internal solitary waves in triggering near-bed mixing in a similar way as what has been shown by Hosegood et al. (2004) for the Faeroe–Shetland Channel. Furthermore, from the observations of current velocity on day 223 it appears that other short mechanisms with different characteristics (no vertical velocity, no rotor) may cause resuspension of loose material. The forcing for those mechanisms remains unclear as it rather appears to be forced by atmospheric lows in the FSC but rather forced by the tide in the deep Rockall Channel. However, both data sets tend to show how the nature of the abrupt current changes rather than their magnitude alone are of key importance to the resuspension process.

Acknowledgement

References

Auffret, G., Khripounoff, A., Vangriesheim, A., 1994. Rapid post-bloom resuspension in the northeastern Atlantic. Deep-Sea Res., Part 1, Oceanogr. Res. Pap. 5/6, 925–939.

Barnett, P.R., Watson, O.J., Connelly, D., 1984. A multiple corer for taking virtually undisturbed samples from shelf, bathyal and abyssal sediments. Oceanol. Acta 7, 399–408.

Beaulieu, S., Baldwin, R., 1998. Temporal variability in currents and the benthic boundary layer at an abyssal station off central California. Deep-Sea Res., Part 2, Top. Stud. Oceanogr. 45, 587–615.

Beaulieu, S.E., Smith Jr., K.L., 1998. Phytodetritus entering the benthic boundary layer and aggregated on the sea floor in the abyssal NE Pacific: macro- and microscopic composition. Deep-Sea Res.: Part 1. Oceanogr. Res. Pap. 45, 781–815.

Bett, B.J., 2001. UK Atlantic margin environmental survey: introduction and overview of bathyal benthic ecology. Cont. Shelf Res. 21, 917–956.

Biscaye, P.E., Anderson, R.F., 1994. Fluxes of particulate matter on the slope of the southern Middle Atlantic Bight: SEEP-II. Deep-Sea Res.: Part 2. Top. Stud. Oceanogr. 41, 459–509.

Boegman, L., Ivey, G.N., Imberger, J., 2005. The degeneration of internal waves in lakes with sloping topography. Limnol. Oceanogr. 50 (5), 1620–1637.

Bonnin, J., van Raaphorst, W., 2004. Dissolved silica enrichment in the deep waters of the Faeroe–Shetland Channel. Deep-Sea Res.: Part 1, Oceanogr. Res. Pap. 51, 1493–1515.

Bonnin, J., van Raaphorst, W., Brummer, G.-J.A., van Haren, H., Malschaert, H., 2002. Intense mid-slope resuspension of particulate matter in the Faeroe–Shetland Channel: short-term deployment of near-bottom sediment traps. Deep-Sea Res.: Part 1. Oceanogr. Res. Pap. 49, 1485–1505.

Bonnin, J., Koning, E., Epping, H.G., Brummer, G.-J., Grutters, M., 2005. Geochemical characterization of resuspended sediment on the southeast slope of the Faeroe–Shetland Channel. Mar. Geol. 214, 215–233.

Bunt, J.A.C., Larcombe, P., Jago, C.F., 1999. Quantifying the response of optical backscatter devices and transmissometers to variations in suspended particulate matter. Cont. Shelf Res. 19, 1199–1220.

Butman, C.A., 1986. Sediment trap biases in turbulent flows: results from a laboratory flume study. J. Mar. Res. 44 (3), 645–693.

Butman, C.A., Grant, W.D., Stolzenbach, K.D., 1986. Predictions of sediment trap biases in turbulent flows: a theoretical analysis based on observation from the literature. J. Mar. Res. 44 (3), 601–644.

Cacchione, D.A., Pratson, L.F., Ogston, A.S., 2002. The shaping on continental slopes by internal tides. Science 296, 724–727.

Durrieu de Madron, X., Radakovitch, O., Heussner, S., Loye-Pilot, M.D., Monaco, A., 1999. Role of the climatological and current variability on shelf-slope exchanges of particulate matter: evidence from the Rhone continental margin (NW Mediterranean). Deep-Sea Res.: Part 1. Oceanogr. Res. Pap. 46 (9), 1513–1538.

Ellett, D.J., Martin, J.H.A., 1973. The physical and chemical oceanography of the Rockall Channel. Deep-Sea Res. 20, 585–625.

Ellett, D.J., Edwards, A., Bowers, R., 1986. The hydrography of the Rockall Channel: an overview. Proc. R. Soc. Edinb. 88B, 61–81.

Gardner, W.D., 1985. The effect of tilt on sediment trap efficiency. Deep-Sea Res. 32 (3), 349–361.

Gardner, W.D., 1989. Periodic resuspension in Baltimore Canyon by focusing of internal waves. J. Geophys. Res. 94, 18185–18194.

Gardner, W.D., Biscaye, P.E., Richardson, M.J., 1997. A sediment trap experiment in the Vema Channel to evaluate the effect of horizontal particle fluxes on measured vertical fluxes. J. Mar. Res. 55, 995–1028.

Gemmrich, J.R., van Haren, H., 2001. Thermal fronts generated by internal waves propagating obliquely along the continental slope. J. Phys. Oceanogr. 31, 649–655.

Gust, G., Michaels, A.F., Johnson, R., Deuser, W.G., Bowles, W., 1994. Mooring line motions and sediment trap hydromechanics: in situ intercomparison of three common deployment designs. Deep-Sea Res.: Part 1. Oceanogr. Res. Pap. 41, 831–857.

Gust, G., Bowles, W., Giordano, S., Hüttel, M., 1996. Particle accumulation in a cylindrical sediment trap under laminar and turbulent steady flow: an experimental approach. Aquat. Sci. 58, 297–326.

Hosegood, P., van Haren, H., 2004. Near-bed solibores over the continental slope in the Faeroe–Shetland Channel. Deep-Sea Res., Part 2, Top. Stud. Oceanogr. 51, 2943–2971.

Hosegood, P., Bonnin, J., van Haren, H., 2004. Solibore-induced resuspension in the Faeroe–Shetland Channel. Geophys. Res. Lett. 31, LO9301. doi:10.1029/2004GL019544.

Kenyon, N.H., 1986. Evidence form bedforms for a strong poleward current along the upper continental slope of NW Europe. Mar. Geol. 72, 187–198.

Klitgaard, A.B., Tendal, O.S., Westerberg, H., 1997. Mass occurrence of large sponges (Porifera) in Faeroe Island (NE Atlantic) shelf and slope areas: characteristics, distribution and possible causes.

In: Hawkins, L.E., Hutchins, S. (Eds.), The Responses of Marine Organisms to their Environments. Southampton Oceanographic Centre, University of Southampton, Southampton, pp. 129–142.

Konert, M., Vandenberghe, J., 1997. Comparison of laser grain size analysis with pipette and sieve analysis: a solution for the underestimation of the clay fraction. Sedimentology 44, 523–535.

Lampitt, R.S., 1985. Evidence for the seasonal deposition of detritus to the deep-sea floor and its subsequent resuspension. Deep-Sea Res. 32 (8), 885–897.

Lampitt, R.S., Newton, P.P., Jickells, T.D., Thompson, J., King, P., 2000. Near-bottom particles flux in the abyssal northeast Atlantic. Deep-Sea Res.: Part 2. Top. Stud. Oceanogr. 47, 2051–2071.

Lonsdale, P., Hollister, C.D., 1979. A near-bottom traverse of the Rockall Trough: hydrographic and geologic inferences. Oceanol. Acta 2, 91–105.

Lynch, J.F., Irish, J.D., Sherwood, C.R., Agrawal, Y.C., 1994. Determining suspended sediment particle size information from acoustical and optical backscatter measurements. Cont. Shelf Res. 14, 1139–1165.

Masson, D.G., Bett, B.J., Billet, D.S.M., Jacobs, C.L., Wheeler, A.J., Wynn, R.B., 2003. The origin of deep-water, coral-topped mounds in the northern Rockall Trough, Northeast Atlantic. Mar. Geol. 194, 159–180.

McPhee-Shaw, E.E., Sternberg, R.W., Mullenbach, B., Ogston, A.S., 2004. Observations of intermediate nepheloid layers on the north California continental margin. Cont. Shelf Res. 24, 693–720.

Monaco, A., Courp, T., Heussner, S., Carbonne, J., Fowler, S.W., Deniaux, B., 1990. Seasonality and composition of particulate fluxes during ECOMARGE-I, western Gulf of Lions. Cont. Shelf Res. 10, 959–987.

New, A.L., Barnard, S., Hermann, P., Molines, J.-M., 2001. On the origin and pathway of the saline inflow to the Nordic Seas: insights from models. Prog. Oceanogr. 48, 255–289.

New, A.L., Smythe-Wright, D., 2001. Aspects of the circulation in the Rockall Trough. Cont. Shelf Res. 21, 777–810.

Oey, L.-Y., 1998. Eddy energetics in the Faeroe–Shetland channel: a model resolution study. Cont. Shelf Res. 17 (15), 1929–1944.

Palanques, Puig, P., Guillén, J., Jiménez, J., Gracia, V., Sánchez-Arcilla, A., Madsen, O., 2002. Near-bottom suspended sediment fluxes on the microtidal low-energy Ebro continental shelf (NW Mediterranean). Cont. Shelf Res. 22, 285–303.

Puig, P., Palanques, A., Guillén, J., 2001. Near-bottom suspended sediment variability caused by storms and near-inertial internal waves on the Ebro mid continental shelf (NW Mediterranean). Mar. Geol. 178, 81–93.

Stoker, M.S., 1995. The influence of glacigenic sedimentation on slope-apron development on the continental margin of Northwest Britain. In: Scrutton, R.A., Stoker, M.S., Shimmield, G.B., Tudhope, A.W. (Eds.), The Tectonics, Sedimentation and Paleoceanography of the North Atlantic Region, Geological Society Special Publication vol. 90. The Geological Society, London.

Thomsen, L., van Weering, T.C.E., 1998. Spatial and temporal variability of particulate matter in the benthic boundary layer at the N.W. European continental margin (Goban Spur). Prog. Oceanogr. 42, 61–76.

Thomsen, L., Gust, G., 2000. Sediment erosion thresholds and characteristics of resuspended aggregates on the western European continental margin. Deep-Sea Res.: Part 1. Oceanogr. Res. Pap. 47 (10), 1881–1897.

Thorpe, S.A., Brubaker, J.M., 1983. Observations of sound reflection by temperature microstructure. Limnol. Oceanogr. 28 (4), 601–613.

Thorpe, S.A., White, M., 1988. A deep intermediate nepheloid layer. Deep-Sea Res. 35 (9), 1665–1671.

US-GOFS, 1989. Sediment trap technology and sampling. In: Knauer, G., Asper, V. (Eds.), Report of the US-GOFS Working Group on Sediment Trap Technology and Sampling, Planning Report, vol. 10. US GOFS Planning Office, Woods Hole, MA. 94 pp.

van Aken, H.M., Becker, G., 1996. Hydrography and through flow in the north-eastern North Atlantic Ocean: the NANSEN project. Prog. Oceanogr. 38, 297–346.

van Haren, H., Groenewegen, R., Laan, M., Koster, B., 2001. A fast and accurate thermistor string. J. Atmos. Ocean. Technol. 18, 256–265.

van Raaphorst, W., Malschaert, H., van Haren, H., Boer, W., Brummer, G.-J., 2001. Cross-slope zonation of erosion and deposition in the Faeroe–Shetland Channel, North Atlantic Ocean. Deep-Sea Res.: Part 1. Oceanogr. Res. Pap. 48 (2), 567–591.

van Weering, T.C.E., McCave, I.N., De Stigter, H.C., Hall, I., Thomsen, L., 1998. Recent sediments, sediment accumulation and carbon burial at Goban Spur, N.W. European continental margin. Prog. Oceanogr. 42, 5–35.

Walsh, I., Fisher, K., Murray, D., Dymond, J., 1988. Evidence for resuspension of rebound particles from near-bottom sediment traps. Deep-Sea Res. 35 (1), 59–70.